

## Proteomic analysis of temperature-dependent developmental plasticity within the ventricle of juvenile Atlantic salmon (*Salmo salar*)

Carlie A. Muir, Bradley S. Bork, Bryan D. Neff, Sashko Damjanovski \*

Department of Biology, Western University, London, ON, Canada

### ARTICLE INFO

#### Keywords:

Thermal plasticity  
Heart  
Proteome  
Mass spectrometry  
Salmonid

### ABSTRACT

In teleosts, cardiac plasticity plays a central role in mediating thermal acclimation. Previously, we demonstrated that exposure to elevated temperatures throughout development (+4°C) improved acute thermal tolerance of the heart in juvenile Atlantic salmon. Fish raised in a warmer thermal regime also displayed higher proportions of compact myocardium within their ventricles. In the present study, we investigated the molecular mechanisms supporting this temperature-specific phenotype by comparing relative protein abundance in ventricular tissue from the same experimental fish using mass spectrometry. We provide the first description of the ventricular proteome in juvenile Atlantic salmon and identify 79 proteins displaying differential abundance between developmental treatments. The subset of proteins showing higher abundance in fish raised under elevated temperatures was significantly enriched for processes related to ventricular tissue morphogenesis, and changes in protein abundance support a hypertrophic model of compact myocardium growth. Proteins associated with the vasculature and angiogenesis also showed higher abundance in the warm-developmental group, suggesting capillarization of the compact myocardium in the hearts of these fish. Proteins related to oxidative metabolism and protein homeostasis also displayed substantive shifts in abundance between developmental treatments, underscoring the importance of these processes in mediating thermal plasticity of cardiac function. While rapid growth under warm developmental temperatures has been linked to cardiomyopathies in farmed salmon, markers of cardiac pathology were not implicated in the present study. Thus, our findings offer a molecular footprint for adaptive temperature-dependent plasticity within the ventricle of a juvenile salmonid.

### 1. Introduction

The teleost heart is a highly plastic organ capable of remodelling to meet altered demands for internal oxygen transport. Cardiac remodelling is observed in response to both physiological and environmental stressors, such as sexual maturation (Graham and Farrell, 1992), exercise training (Castro et al., 2013; Dindia et al., 2017; Gallaughier et al., 2001), anemia (Simonot and Farrell, 2007), hypoxia (Anttila et al., 2015), and thermal acclimation (Jayasundara et al., 2015; Keen et al., 2016; Klaiman et al., 2011; Vornanen et al., 2005). Indeed, cardiac function is considered an important mediator of thermal tolerance in many fishes. As tissue oxygen demands change with environmental temperature, cardiac plasticity facilitates compensatory changes that reduce temperature-induced mismatches between oxygen supply and demand (Farrell et al., 2009; Pörtner and Knust, 2007). The capacity for cardiac plasticity is enhanced in fish which occupy relatively wide thermal ranges, such as temperate species. Indeed, cardiac plasticity

allows many temperate fishes to remain active throughout seasonal temperature fluctuations. Plasticity in acute thermal tolerance of the heart is also critical, as the heart is the first organ to fail in fish exposed to heat stress (Iftikar and Hickey, 2013). It is therefore important to understand the mechanisms that preserve cardiac function during heat stress in fish, particularly as anthropogenic climate change increases both average seasonal temperatures and the frequency of severe heat-waves (IPCC, 2021).

At elevated temperatures, convective transport of blood by the heart must increase to meet heightened tissue oxygen demands, while aerobic demands of the heart itself also increase (Eliason and Anttila, 2017). In salmonids, plastic adjustments to increased environmental temperatures often increase cardiac capacity and oxygenation of the myocardium (Anttila et al., 2014, 2015; Jørgensen et al., 2014; Muñoz et al., 2015). This plasticity can involve a reorganization of the excitation, contractile, and metabolic machinery within cardiomyocytes, as well as gross tissue morphogenesis within the cardiovascular system (Anttila et al., 2015;

\* Corresponding author.

E-mail address: [sdamjano@uwo.ca](mailto:sdamjano@uwo.ca) (S. Damjanovski).

<https://doi.org/10.1016/j.crphys.2022.07.005>

Received 12 November 2021; Received in revised form 20 July 2022; Accepted 29 July 2022

Available online 10 August 2022

2665-9441/© 2022 The Authors. Published by Elsevier B.V. This is an open access article under the CC BY-NC-ND license (<http://creativecommons.org/licenses/by-nc-nd/4.0/>).

Hassinen et al., 2008; Keen et al., 2017; Klaiman et al., 2011; Shiels et al., 2011; Vornanen et al., 2002). In addition to the heart's role in compensating for oxygen-limitation at supra-optimal temperatures, cardiomyocytes must also contend with direct temperature effects on protein integrity and cell homeostasis. Previous studies have implicated heat shock proteins and the oxidative stress response as important mediators of thermal stress across teleosts, from highly eurythermal goby fish to the extremely stenothermic notothenioid fishes (Anttila et al., 2014; Beemelmanns et al., 2021a, 2021b; Jayasundara et al., 2015; Jeffries et al., 2014; Jørgensen et al., 2014; Logan and Somero, 2011; O'Brien et al., 2018; Podrabsky and Somero, 2004).

In fish, chronic changes in temperature often affect relative heart size, as well as the ratio of spongy to compact myocardium within the ventricle. In highly active fishes, such as salmonids, the ventricle consists of a highly-trabeculated spongy myocardium that spans the inner lumen and is encased by an outer compact myocardium (Davie and Farrell, 1991; Tota, 1983). While a coronary blood supply perfuses the outer compact myocardium, the spongy myocardium receives oxygen from venous blood inside the lumen of the ventricle (Davie and Farrell, 1991). In salmonids, relative ventricle mass tends to increase during cold-acclimation, along with the relative proportion of spongy myocardium (Farrell et al., 1988; Klaiman et al., 2011). This is thought to increase stroke volume, thereby compensating for temperature-related decreases in heart rate. Conversely, the proportion of compact myocardium tends to increase following warm-acclimation (Anttila et al., 2015; Keen et al., 2016; Klaiman et al., 2011), as well as capillary density within the compact myocardium (Anttila et al., 2015). This change has been posited as a compensatory response to oxygen-limitation within the myocardium itself at supra-optimal temperatures (Ekström et al., 2017; Farrell et al., 1996). In Atlantic salmon, temperature-induced proliferation of the compact myocardium is not observed when the acclimation temperature exceeds 19°C, suggesting that cardiac remodelling may be constrained above a species-specific temperature threshold (Gamperl et al., 2020).

In fish, compensatory cardiac growth is facilitated through a combination of myocyte growth (hypertrophy) and proliferation (hyperplasia) (Gamperl and Farrell, 2004). This combination is in contrast to the mammalian heart, which can only grow via cardiac hypertrophy after development. Cardiac hypertrophy can be characterized as either 'physiological/adaptive hypertrophy' or 'pathological hypertrophy', depending on the underlying stimulus, resulting morphology, and functional outcomes. Cardiac hypertrophy is triggered by increased biomechanical strain on cardiomyocytes, resulting from chronic increases in volume and/or pressure load (Bernardo et al., 2010). In mammals, volume overloading often occurs as a result of heightened aerobic demands, such as during exercise-training. This triggers physiological hypertrophy, where increases in ventricular wall thickness are proportional to chamber volume and lead to enhanced pumping capacity (Bernardo et al., 2010). Conversely, pathological stressors such as disease and hypertension can cause chronic pressure overloading and result in aberrant cardiac growth. Pathological hypertrophy is characterized by a disproportionate thickening of the ventricular wall that increases stiffness and encroaches on luminal volume, leading to impaired pumping capacity (Bernardo et al., 2010). Physiological and pathological hypertrophy also differ in their associated molecular markers. In mammals, pathological cardiac hypertrophy is typified by the re-expression of embryonic gene programs, including atrial natriuretic peptide (ANP), brain natriuretic peptide (BNP), and regulator of calcineurin 1 (RCAN1). Functionally, thermal remodelling of the teleost heart is considered analogous to physiological remodelling of the mammalian heart (Keen et al., 2016). However, a recent study in farmed Atlantic salmon found that rapid development under elevated temperatures was associated with increased levels of cardiac pathology markers and aberrant hypertrophic growth of the compact myocardium (Frisk et al., 2020). Thus, there is a need to further explore adaptive versus pathological remodelling of the teleost heart in response to

environmental temperature, as well as the underlying molecular mechanisms.

We previously showed that a 4°C increase in developmental temperature enabled juvenile Atlantic salmon (*Salmo salar*) to maintain cardiac function to temperatures approximately 2°C higher than control fish (Muir et al., 2021a). The proportion of compact myocardium in the ventricles of fish reared under elevated temperatures was also 70% greater than in control fish. Here, we investigate the molecular mechanisms underlying the observed differences in myocardial structure and thermal performance by performing a global proteomic analysis on ventricular tissue from the same experimental fish. While our thermal performance findings suggest adaptive temperature-dependent plasticity in the heart, we also sought to determine whether these fish would display molecular signatures of pathological cardiac remodelling.

## 2. Materials and methods

### 2.1. Animal rearing

The rearing protocol used here is detailed in Muir et al. (2021a) and all experiments were carried out according to Western University Animal Care protocol 2018-084. Briefly, fertilized Atlantic salmon embryos were obtained from the Ontario Ministry of Natural Resources and Forestry's Normandale Research Facility (Vittoria, Ontario) and transported to a hatchery facility at Western University (London, Ontario) 24 h after fertilization. Here, embryos were divided between vertical egg tray incubators that corresponded to two temperature treatments: control (+0°C) or elevated (+4°C) temperatures. Water supplying the +0°C incubator was maintained at  $7 \pm 0.5^\circ\text{C}$  while the +4 incubator was maintained at  $11 \pm 0.5^\circ\text{C}$ . When hatched fry approached full absorption of their endogenous yolk sacs (approximately 4 months for +0-fish and 2.5 months for +4-fish), they were transferred to 40 L tanks and rearing temperatures were raised by 4°C in each treatment to mimic the seasonal temperature increase that cues a transition to exogenous feeding. Juvenile fish were provided with pelleted feed ad libitum and maintained under these conditions (rearing temperature of 11°C for the +0-treatment and 15°C for the +4-treatment) until thermal performance trials were performed in yearlings (1+).

### 2.2. Temperature ramping and sample collection

We determined cardiorespiratory thresholds for thermal performance in the two developmental treatments by measuring the response of pharmacologically stimulated maximum heart rate ( $f_{H\max}$ ) to acute warming using noninvasive Doppler echocardiography in anaesthetized juveniles, according to Muir et al. (2021b). In these thermal performance trials, temperature was increased at a rate of  $10^\circ\text{C h}^{-1}$  until the onset of cardiac arrhythmias, starting from the fish's respective rearing temperatures (11°C for +0-fish and 15°C for +4-fish; Muir et al., 2021a).  $T_{\text{Arr}}$ , the temperature at which the heart becomes arrhythmic, signifies the upper thermal limit for cardiac performance. On average, trials lasted between 60 and 90 min from the start of temperature ramping to the onset of cardiac arrhythmias. Once  $T_{\text{Arr}}$  was reached, fish were euthanized by lethal overdose of MS-222 and the ventricle was removed from a subset of fish for use in the present study. In the subset of fish used for mass spectrometry ( $N = 3$  per treatment),  $T_{\text{Arr}}$  was significantly higher in fish from the +4-treatment, with a mean of  $27.7 \pm 2.1^\circ\text{C}$  compared to  $22.50 \pm 0.9^\circ\text{C}$  in the +0-treatment ( $t_4 = 4.0$ ,  $p = 0.02$ ; unpaired Student's *t*-test).

Each ventricle was rinsed twice with PBS to remove excess blood and immediately placed in 500 µl of TRIzol Reagent (ThermoFisher) in a 1.5 mL Eppendorf Safe-Lock microcentrifuge tube, then manually trimmed with sterilized dissection scissors. Approximately 50 µl of 1 mm zirconium silicate beads (Next Advance) were then added to the microcentrifuge tube and the sample was homogenized in a Next Advance Bullet Blender for 2 min at maximum speed. Beads were separated from

the lysate by centrifugation  $12\,000\times g$  for 5 min and the supernatant was transferred to a fresh microcentrifuge and stored at  $-80^{\circ}\text{C}$ .

### 2.3. Protein isolation and sample preparation for mass spectrometry

Proteins were isolated from the TRIzol supernatant according to the manufacturer's instructions and the protein pellet was resuspended in 8 M urea. Protein in 8 M urea was quantified via Bradford Assay and 100  $\mu\text{g}$  of total protein was diluted to 1 M urea (pH 8–9) by adding 50 mM ammonium bicarbonate. Samples were dried in a speed vac (1–1.5 h) and reconstituted in 44  $\mu\text{L}$  of 50 mM ammonium bicarbonate. Cysteine residues were reduced with 1  $\mu\text{L}$  of 100 mM TCEP-HCl and shaken at  $37^{\circ}\text{C}$  for 1 h. Samples were cooled to room temperature before cysteine residues were alkylated with 1  $\mu\text{L}$  500 mM iodoacetamide and shaken at room temperature and in dark for 45 min. Samples were digested overnight at  $37^{\circ}\text{C}$  with 1  $\mu\text{g}$  Trypsin. The reaction was stopped with 2  $\mu\text{L}$  acetic acid. The final volume was 50.5  $\mu\text{L}$ . The resulting peptide samples were desalted using C-18 ZipTips (Millipore, ZTC18M960). Peptides were eluted with 70% acetonitrile and 0.1% formic acid and dried.

### 2.4. LC-MS/MS data collection

Label-free quantitative proteomics was performed on three biological replicates per treatment at the Donnelly Mass Spectrometry Facility (University of Toronto), with each biological replicate run in triplicate. Peptides were analyzed by liquid chromatography – tandem mass spectrometry (LC-MS/MS) on an EASY-nLC 1200 system (ThermoFisher Scientific) coupled to a Q Exactive HF mass spectrometer (ThermoFisher Scientific).

Dried samples were reconstituted in 20 mL of 1% formic acid and 5 mL was trapped within an Acclaim PepMap Trap Column (100  $\text{\AA}$ , 3  $\mu\text{m}$ , 75  $\mu\text{m} \times 20\text{ mm}$ ; 164 946, Thermo Fisher). After trapping, peptides were separated using an Acclaim PepMap analytical column (100  $\text{\AA}$ , 2  $\mu\text{m}$ , 75  $\mu\text{m} \times 500\text{ mm}$ ; ES803A, Thermo Fisher). Buffer A contained 0.1% formic acid in water. Buffer B contained 80% acetonitrile in 0.1% formic acid. The separation was performed in 180 min at a flow rate of 220 nL/min, with a gradient of 5%–25% buffer B in 155 min, following by 25%–100% in 9 min, and 100% buffer B for 15 min. Eluted peptides were directly sprayed into a Q Exactive HF Mass spectrometer (ThermoFisher Scientific) with collision induced dissociation (CID) using a nanospray ion source (Proxeon). The mass spectrometer was controlled by Xcalibur software (ThermoFisher Scientific) and operated in data-dependent mode. MS scans recorded the mass-to-charge ( $m/z$ ) of ions over a range of 300–1650 with a resolution of 60 000 (MS) or 15 000 (MS/MS) FWHM (full width half maximum) and a target of  $3 \times 10^6$  (MS) or  $1 \times 10^5$  (MS/MS) ions. The 20 most intense multiply charged ions (+2 to +7 charged states) were automatically selected for collision-induced association in the ion trap with an isolation width of 1.4  $m/z$  and a 0.0  $m/z$  offset.

### 2.5. LC-MS/MS data processing

Identification and quantification of cardiac proteins was performed using MaxQuant version 1.6.6.0 against the UniProt Atlantic salmon (*Salmo salar*) database (downloaded February 19, 2020) with enzyme specificity for trypsin. The mass tolerances were 20 ppm for precursor ions and 4.5 ppm for fragment ions. Carbamidomethylation of cysteine residues was considered a fixed modification, whereas oxidation of methionine residues and acetylation on protein N-termini were considered variable modifications. Search parameters allowed up to two missed tryptic cleavages. A high confidence in the peptide-protein identifications was assured by using a PSM (peptide-to-spectrum match) FDR and protein FDR of 0.01 (1%).

### 2.6. Differential protein abundance analysis

Raw MaxQuant outputs were imported into the MSqRob Shiny App (run via R) for differential quantitative analysis between the developmental treatments using a peptide-based model, which has been shown to uniformly outperform summarization-based models (Sticker et al., 2020). Data were analyzed following the default MSqRob pipeline described in Goeminne et al. (2018). Briefly, data were  $\log_2$ -transformed and a quantile normalization was applied. The dataset was filtered to remove razor peptides that could not be uniquely attributed to a single protein or protein group, proteins that were only identified by a modification site, contaminants, and reversed sequences. The 'minimum number of times a peptide sequence should be identified' was set to two, thereby removing peptides that were only observed once across all samples. Thus, a protein identified by only one peptide can contribute to the quantitative estimation, provided that the peptide is identified in multiple samples (Goeminne et al., 2018). Finally, treatments in which a protein was only observed in one biological replicate were still included in the differential quantitative analysis for this protein (Sticker et al., 2020). For the differential analysis, developmental treatment was included as a fixed factor in the model, while sequence, biological replicate, and technical replicate were included as random factors. P-values were adjusted for multiple testing using the Benjamini–Hochberg False Discovery Rate (FDR) procedure, and the FDR threshold was set to 5%.

### 2.7. Bioinformatics analysis

Protein ontology of the ventricle proteome was conducted for all identified proteins using Blast2GO (Götz et al., 2008). Protein sequences were BLASTp searched against the mammalian (taxa: 40674) NCBI non-redundant protein database (June 2021) to obtain gene ontology (GO) terms, which were then filtered against *Actinopterygii* (taxa: 7898) to remove any terms that are incompatible with bony fishes. GO enrichment analysis using Fisher's exact test was performed. Differentially abundant proteins were used as the test list while all other identified proteins within the dataset were used as the reference list. GO terms were filtered to display only the most specifically enriched child terms while excluding more general parent terms. Results were further filtered to only include GO terms with  $\geq 2$  associated proteins within the test list.

Gene set enrichment analysis (GSEA) was additionally performed using the t-statistics for differential protein abundance computed by MSqRob. The permutation number was set at 1000 and significance was accepted at an FDR  $\leq 0.05$ . As above, enriched pathways were further filtered to display only most specifically enriched child terms.

### 2.8. Western blotting

Remaining protein lysate from samples submitted for mass spectrometry was subsequently used for immunoblot analysis ( $N = 3$  per treatment). However, one sample from the warm-developmental group had insufficient sample volume following mass spectrometry and was therefore replaced by another ventricular protein sample from the same treatment group. Samples (10  $\mu\text{g}$ ) were diluted with Laemmli's buffer (BioRad), boiled for 5 min, and loaded onto a 15% polyacrylamide gel and separated by SDS-PAGE. Separated proteins were transferred onto a polyvinylidene difluoride (PVDF) membrane (BioRad) overnight at  $4^{\circ}\text{C}$  using 12 V. Membranes were blocked in 5% bovine serum albumin (BSA) dissolved in tris-buffered saline with 0.05% Tween-20 (TBST) overnight at  $4^{\circ}\text{C}$ . Blots were then incubated overnight at  $4^{\circ}\text{C}$  with a primary antibody, followed by goat anti-rabbit secondary antibody (1:10 000 in 5% blocking buffer; 1 706 515; BioRad) for 1 h at room temperature. Blots were visualized using a ChemiDoc Imaging System (BioRad) and densitometry was performed using Image Lab 6.0.1 (BioRad).

Mammalian antibodies were used to confirm patterns in differential

abundance between developmental groups for two proteins detected by mass spectrometry (Supplemental Materials). A rabbit anti-CIAPIN1 polyclonal antibody (0.2 µg/mL in 5% blocking buffer; NBP1-89096; Novus Biologicals) was developed against a recombinant protein sequence with 76% similarity to the *S. salar* ortholog anamorsin (E value =  $5 \times 10^{-42}$ ). A rabbit anti-myosin light chain 1-3 polyclonal antibody (0.2 µg/mL in 5% blocking buffer; NBP2-57186; Novus Biologicals) was developed against a recombinant sequence with 77% similarity to the *S. salar* ortholog myosin light chain 1-1 (E value =  $1 \times 10^{-11}$ ). Amido black was used to stain total protein on transferred membrane blots. Anamorsin and myosin light chain 1-1 abundance was

standardized against total protein and normalized to the control (+0) group. Protein abundance was compared between developmental groups using an unpaired Student's t-test ( $\alpha = 0.05$ ).

### 3. Results

#### 3.1. Summary of the ventricular proteome

Mass spectra were searched against the UniProt database, and 2310 proteins were identified across both developmental groups of juvenile Atlantic salmon. Proteins were categorized based on biological process,

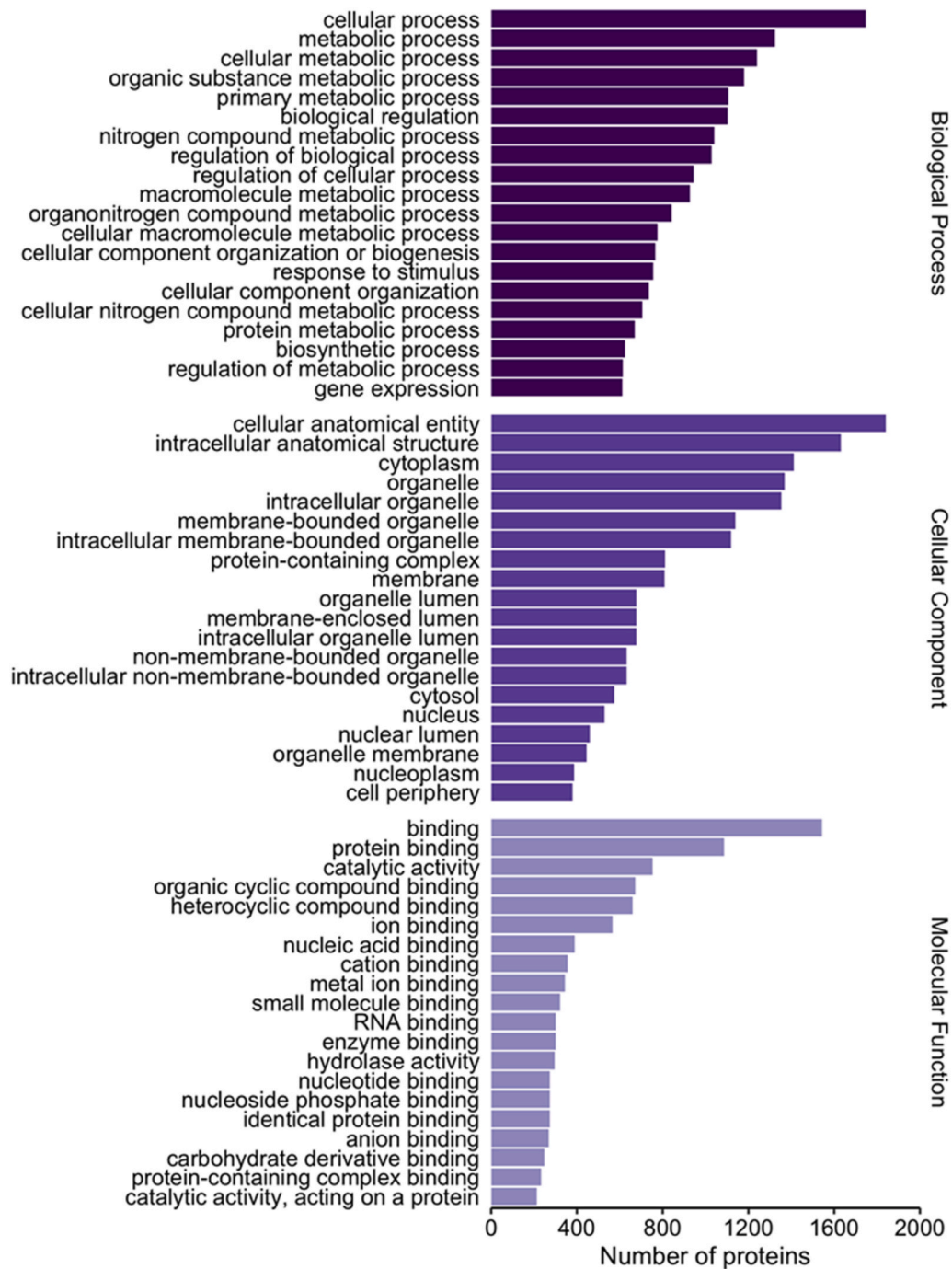


Fig. 1. Gene ontology (GO) distribution of the 2310 proteins quantified in both control (+0) and treatment (+4) Atlantic salmon (*Salmo salar*) ventricles. Mass spectra data were searched against the *Salmo salar* proteome in the Uniprot database. The top 20 GO terms for biological process, cellular compartment, and molecular function are presented.

cellular component, and molecular function via protein ontology analysis in Blast2GO, with the top 20 subcategories displayed in Fig. 1. Cellular and metabolic processes were the most common biological processes, while binding-related functions dominated the molecular function category. The top subcategories for cellular component were cellular anatomical entities and intracellular anatomical structures.

### 3.2. Differential protein abundance in juvenile Atlantic salmon raised in two thermal regimes

We identified 79 proteins that showed differential abundance in the ventricular tissue of fish from the two developmental treatments (Supplemental Materials). Enrichment analysis of all differentially abundant proteins revealed enrichment for several biological processes related to muscle contraction (Fig. 2A). Indeed, terms related to the troponin complex were enriched in both the cellular component and molecular function categories.

Among the differentially abundant proteins, 43 showed higher abundance in the +4-group, which was exposed to elevated temperatures during development. Notably, this subset of proteins was enriched for biological processes related to ventricular tissue morphogenesis and mitochondrial electron transport (Fig. 2B). The mitochondrial respiratory chain (complex III) was further implicated as an enriched cellular component, while molecular functions pertaining to metal ion binding and structural constituents of muscle were enriched in the molecular function category.

The subset of proteins showing lower abundance in +4-fish relative

to controls (36 proteins) was enriched for biological processes related to apoptosis, secondary alcohol metabolism, and protein ubiquitination (Fig. 2C). Protein ubiquitination was further implicated within this subset of proteins by enrichment of ubiquitin-protein transferase activity in the molecular function category.

We further investigated trends in differential protein expression between developmental treatments using gene set enrichment analysis (GSEA; Fig. 3), which identifies overrepresented pathways within the ranked list of differentially abundant proteins. Among the proteins showing higher abundance in the +4-group, GSEA revealed significant enrichment for terms related to mitochondria, specifically, the electron transport chain. For proteins showing lower abundance in the +4-group, GSEA revealed enrichment for terms related to the endopeptidase complex and carbohydrate metabolism.

In addition to the enrichment analyses (Figs. 2 and 3), we manually identified a number of differentially abundant proteins with roles in cell stress, cytoskeleton organization, cell adhesion, cell signaling, and expression. Therefore, we will expand on differentially abundant proteins from six functional categories below: metabolism, muscle contraction, cell integrity, cell stress, tissue morphogenesis, and expression and translation. A selected list of differentially abundant proteins is presented in Table 1.

### 3.3. Metabolism

Several components of the mitochondrial electron transport chain showed increased abundance in the +4-group (Table 1). These proteins

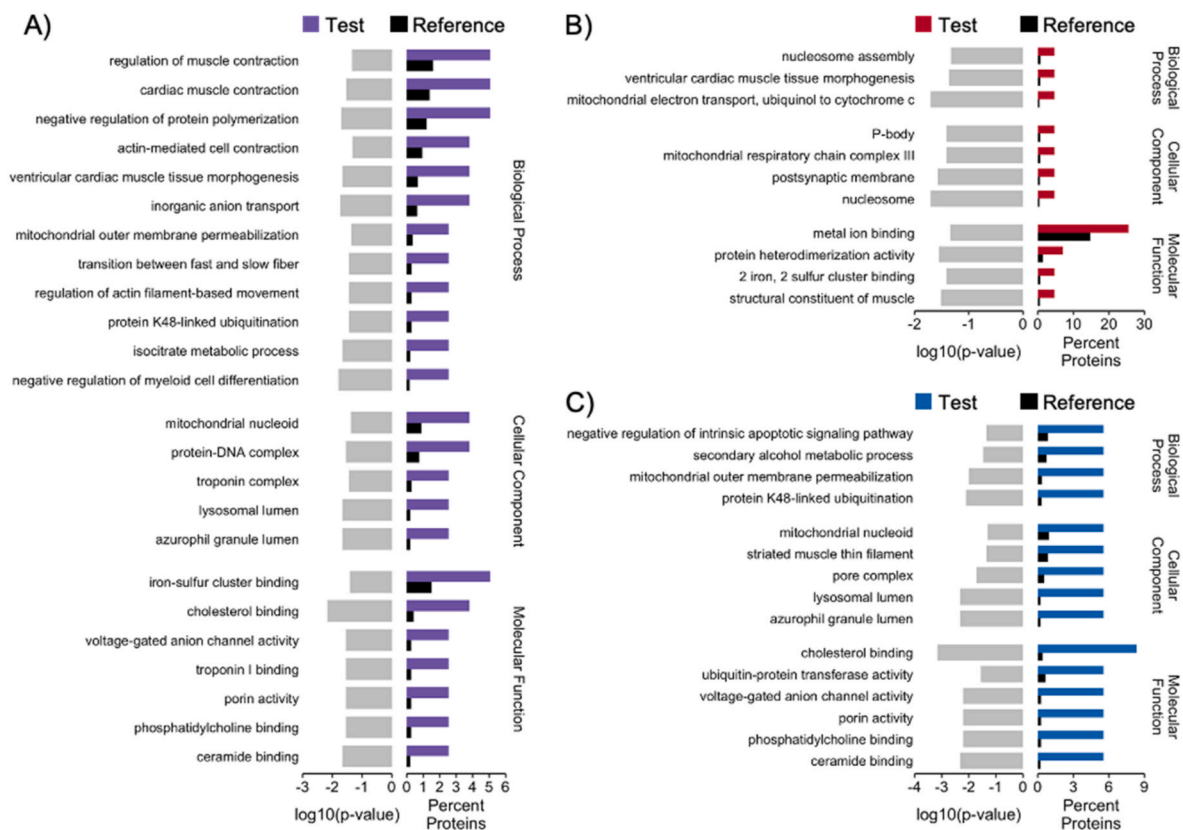


**Fig. 2.** Gene ontology (GO) analysis of differentially abundant proteins in the ventricles of juvenile Atlantic salmon (*Salmo salar*) raised under elevated temperature conditions (+4°C). Bar charts display significantly enriched GO terms (Fisher's exact test,  $p \leq 0.05$ ) with a minimum of 2 associated proteins for each biological process, cellular component, and molecular function. Grey bars indicate significance level ( $\log_{10}(p\text{-value})$ ). Black bars represent the percentage of proteins associated with the GO term in the Reference protein list (not differentially abundant), while A) purple bars indicate the percentage of proteins associated with the GO term in the full Test list of differentially abundant proteins (79 proteins), B) red bars indicate the percentage of proteins associated with the GO term in the Test list of proteins with higher abundance in the +4-treatment relative to the control (+0) treatment (43 proteins), and C) blue bars indicate the percentage of proteins associated with the GO term in the Test list of proteins with lower abundance in the +4-treatment relative to the +0-treatment (36 proteins). (For interpretation of the references to colour in this figure legend, the reader is referred to the Web version of this article.)

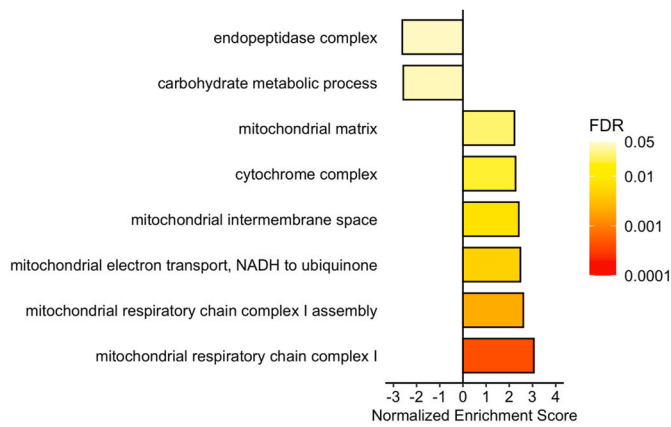


**Fig. 3. Gene set enrichment analysis (GSEA) results from a comparison of ventricular protein abundance in the two developmental treatments (+4 vs. +0).** A positive Normalized Enrichment Score (NES) indicates upregulation in the +4-treatment relative to the control (+0) treatment, while a negative NES value indicates downregulation in the +4-treatment. Colour indicates the degree of significance (FDR q-value). (For interpretation of the references to colour in this figure legend, the reader is referred to the Web version of this article.)

included two subunits of complex III (cytochrome *b-c1* complex subunit 7 and cytochrome *b-c1* complex subunit 1) and one subunit of complex IV (cytochrome *c* oxidase subunit). Two proteins associated with the TCA cycle also displayed increased abundance in the +4-group (aconitate hydratase and 2-oxoglutarate dehydrogenase), while abundance of isocitrate dehydrogenase [NADP] was reduced (Table 1).

Conversely, two proteins associated with carbohydrate metabolism were less abundant in the +4-group (Table 1). Specifically, levels of the glycolytic protein triosephosphate isomerase were lower in the hearts of +4-fish compared to the +0-group, as were levels of alpha-galactosidase – which functions to breakdown oligosaccharides. Abundance of the AMP-salvage enzyme, adenosine kinase, was also reduced in the +4-group.

### 3.4. Muscle contraction

A number of proteins associated with muscle contraction were differentially abundant between the developmental groups (Table 1). With the exception of troponin C, components of the troponin-tropomyosin complex showed increases in the hearts of +4-fish, including tropomyosin alpha-1 (isoform X1), myosin light chain 1 (skeletal muscle isoform-like), and troponin I (slow skeletal muscle-like isoform X1). We observed lower abundance of two proteins associated with sarcomere organization in the +4-group: myozenin 2 and tropomodulin-1-like (isoform X1). Myosin-binding protein H-like (isoform X1), which functions within the cardiac conduction system, also displayed lower abundance in the hearts of +4-fish.

### 3.5. Cell integrity

Common among differentially abundant proteins were those associated with the cytoskeleton and extracellular matrix (Table 1). Three proteins involved in cell adhesion were more abundant in the hearts of +4-fish: dermatopontin-like, collagen type-VIII, and alpha-dystroglycan. Meanwhile, two proteins associated with cell migration (SH3 domain-containing kinase-binding protein 1 and plexin-B2-like) were less abundant in the +4-group.

### 3.6. Cell stress

Among the differentially abundant proteins, many were associated

**Table 1**

Differentially abundant proteins in the ventricles of juvenile Atlantic salmon (*Salmo salar*) raised under elevated temperature conditions (+4°C). A positive Log<sub>2</sub>FC indicates higher abundance in the +4-group relative to control (+0) fish, while a negative Log<sub>2</sub>FC indicates lower abundance in the +4-group. Proteins are ordered by significance based on the FDR q-value within each subcategory.

Protein	Accession	Function	Log <sub>2</sub> FC	q-value
<b>Metabolism</b>				
Cytochrome <i>b-c1</i> complex subunit 7	B5X6V2	Electron transport chain	0.849	4.639 × 10 <sup>-11</sup>
Aconitate hydratase, mitochondrial	A0A1S3SGT2	TCA cycle	3.44	5.934 × 10 <sup>-8</sup>
Adenosine kinase	B5DGF0	AMP salvage	-0.916	7.412 × 10 <sup>-5</sup>
Triosephosphate isomerase	B5XB51	Glycolysis	-0.366	2.882 × 10 <sup>-4</sup>
Cytochrome <i>c</i> oxidase subunit	B5X6I9	Electron transport chain	0.631	2.882 × 10 <sup>-4</sup>
Alpha-galactosidase	C0HA45	Oligosaccharide metabolism	-2.089	0.025
Isocitrate dehydrogenase [NADP]	B5DGS2	TCA cycle	-1.034	0.040
2-oxoglutarate dehydrogenase, mitochondrial isoform X1	A0A1S3PRS0	TCA cycle	0.442	0.044
Cytochrome <i>b-c1</i> complex subunit 1, mitochondrial-like	A0A1S3P342	Electron transport chain	1.033	0.049
<b>Muscle contraction</b>				
Tropomyosin alpha-1 chain isoform X1	A0A1S3KNT1	Muscle contraction	3.802	3.371 × 10 <sup>-9</sup>
Myosin light chain 1, skeletal muscle isoform-like	B5DH12	Muscle contraction	3.691	4.806 × 10 <sup>-7</sup>
Myosin-binding protein H-like isoform X1	A0A1S3LFH7	Conduction regulation	-2.072	1.318 × 10 <sup>-4</sup>
Tropomodulin-1-like isoform X1	A0A1S3SJ69	Sarcomere organization	-0.879	2.101 × 10 <sup>-3</sup>
Myozenin 2	B5DH18	Sarcomere organization	-1.427	0.019
Troponin C, slow skeletal and cardiac muscle-like	A0A1S3LJ89	Muscle contraction	-1.625	0.024
Troponin I, slow skeletal muscle-like isoform X1	A0A1S3P1Y4	Muscle contraction	2.956	0.030
<b>Cell integrity</b>				
Dermatopontin-like	A0A1S3MQE7	Cell adhesion	1.399	7.379 × 10 <sup>-3</sup>
SH3 domain-containing kinase-binding protein 1-like isoform X1	A0A1S3RHE9	Cell migration	-0.563	0.016
Collagen alpha-1 (VIII) chain-like	A0A1S3QWL9	Cell adhesion	1.237	0.030
Plexin-B2-like	A0A1S3N1G1	Cell migration	-0.785	0.040
Alpha-dystroglycan	A0A1S3P849	Cell adhesion	0.585	0.043
<b>Cell stress</b>				
Small glutamine-rich tetratricopeptide repeat-containing protein alpha	B5DGG3	Ubiquitin-dependent protein catabolic process	-1.139	8.200 × 10 <sup>-9</sup>
Zinc-binding protein A33-like	A0A1S3LZC9	Protein ubiquitination	-0.887	3.135 × 10 <sup>-7</sup>

(continued on next page)

**Table 1** (continued)

Protein	Accession	Function	Log <sub>2</sub> FC	q-value
Anamorsin	B5XEX1	Anti-apoptotic	-1.195	4.806 × 10 <sup>-7</sup>
Aminoacyl-tRNA hydrolase	A0A1S3LS03	Pro-apoptotic	-0.781	9.242 × 10 <sup>-6</sup>
CREG1	A0A1S3MTL4	Autophagy regulation	0.959	4.271 × 10 <sup>-4</sup>
Prefoldin subunit 3	B5XA06	Protein folding	-0.742	9.610 × 10 <sup>-4</sup>
Heat shock protein beta-2	A0A1S3QKN9	Response to heat	0.417	7.010 × 10 <sup>-3</sup>
Peroxiredoxin-6-like isoform X1	A0A1S3PAZ6	Cell redox homeostasis	-0.778	7.145 × 10 <sup>-3</sup>
Voltage-dependent anion-selective channel protein 2	B5DH06	Anti-apoptotic	-0.712	0.013
Proteasome subunit beta	A0A1S3RIW7	Protein catabolic process	-1.525	0.014
Heat shock 70 kDa protein 9	C0HAF8	Protein folding	0.681	0.019
Small ubiquitin-related modifier 1	A0A1S3P0T6	Response to heat stress	-2.119	0.024
Ubiquitin-conjugating enzyme E2 H	C0H938	Ubiquitin-dependent protein catabolic process	-0.545	0.024
Selenoprotein M-like	A0A1S3NMW7	Cell redox homeostasis	0.873	0.030
Ubiquitin carboxyl-terminal hydrolase	B9EPR5	Ubiquitin-dependent protein catabolic process	-0.374	0.033
Thioredoxin, mitochondrial-like isoform X1	A0A1S3R9B0	Cell redox homeostasis	1.139	0.037
S-phase kinase-associated protein 1	B5X9I6	Ubiquitin-dependent protein catabolic process	-0.809	0.042
<b>Tissue morphogenesis</b>				
Tetranectin	B5XCV4	Myogenesis	1.593	6.392 × 10 <sup>-5</sup>
Ribonuclease-like 3	A0A1S3RS25	Angiogenesis	0.846	6.392 × 10 <sup>-5</sup>
S100-A16	B5XDV1	Angiogenesis; Cell proliferation	1.443	9.886 × 10 <sup>-4</sup>
Protein-glutamine gamma-glutamyltransferase 2	B5X1F9	Blood vessel remodelling	2.515	0.018
<b>Expression and translation</b>				
Mitochondrial import inner membrane translocase subunit	B5X8D2	Mitochondrial protein transport	1.053	8.200 × 10 <sup>-9</sup>
28S ribosomal protein S14, mitochondrial	B9EN50	Mitochondrial translation	0.654	7.092 × 10 <sup>-3</sup>
Pre-mRNA-splicing factor SPF27	B5XBW1	RNA splicing	-0.636	7.379 × 10 <sup>-3</sup>
40S ribosomal protein S13	A0A1S3KN82	Translation	1.931	0.013
40S ribosomal protein S15a	B5DGX3	Translation	4.380	0.025
G-rich sequence factor 1	A0A1S3M7H9	Regulation of RNA splicing	-1.056	0.033
	A0A1S3T4N9	P-body assembly	0.729	0.046

**Table 1** (continued)

Protein	Accession	Function	Log <sub>2</sub> FC	q-value
U6 snRNA-associated Sm-like protein LSm4				

with cellular stress responses (Table 1). A number of proteins associated with ubiquitin-dependent protein degradation showed decreased abundance in the hearts of +4-fish, including small glutamine-rich tetrapeptide repeat-containing protein alpha, zinc-binding protein A33-like, small ubiquitin-related modifier 1, ubiquitin-conjugating enzyme E2 H, ubiquitin carboxyl-terminal hydrolase, and S-phase kinase-associated protein 1. Proteasome subunit beta and prefoldin (subunit 3), a molecular chaperone which combats protein aggregation, also displayed lower abundances in +4-fish. Conversely, two heat shock chaperones (heat shock protein beta-2 and heat shock 70 kDa protein 9) were more abundant in the +4-group, as well as the autophagy regulator CREG1 (Table 1).

Proteins involved in cellular protection against oxidative stress also displayed differential abundance between developmental groups, with selenoprotein M-like and thioredoxin (mitochondrial-like isoform X1) showing higher abundance in the +4-group, and peroxiredoxin-6-like (isoform X1) showing lower abundance. Finally, three proteins associated with apoptosis displayed lower abundance in the hearts of +4-fish: the anti-apoptotic anamorsin and voltage-dependent anion-selective channel protein 2, and the pro-apoptotic aminoacyl-tRNA hydrolase.

### 3.7. Tissue morphogenesis

A number of cell signaling proteins with roles in tissue morphogenesis were differentially abundant between the developmental groups (Table 1). Notably, three proteins which promote angiogenesis (ribonuclease-like 3 and S100-A16) and blood vessel remodelling (protein-glutamine gamma-glutamyltransferase 2) were more abundant in the +4-group. Tetranectin, a secreted protein associated with myogenesis during embryonic development, also displayed higher abundance in the hearts of +4-fish.

### 3.8. Expression and translation

A number of proteins involved in protein biosynthesis were found to be more abundant in the hearts of +4-fish, including 28S ribosomal protein S14 (mitochondrial), 40S ribosomal protein S13, and 40S ribosomal protein S15 (Table 1). Mitochondrial import inner membrane translocase subunit, associated with protein import into the mitochondria, also showed higher abundance in the +4-group.

Proteins involved in post-transcriptional regulation were also differentially abundant between the developmental groups (Table 1). Two proteins associated with RNA splicing, pre-mRNA-splicing factor SPF27 and G-rich sequence factor 1, were less abundant in the +4-group; while U6 snRNA-associated Sm-like protein LSm4, involved in P-body assembly, was more abundant in the +4-group.

### 3.9. Western blotting

To corroborate differential protein abundance detected by mass spectrometry, we performed Western blotting for myosin light chain 1-1 and anamorsin (Fig. 4). Mass spectrometry identified a greater abundance of myosin light chain 1-1 in the hearts of +4-fish ( $\log_2FC = 3.691$ ;  $q = 4.806 \times 10^{-7}$ ). A similar trend was detected using Western blotting, though the difference between developmental groups did not reach statistical significance ( $\log_2FC = 1.168$ ;  $p = 0.076$ ). Similarly, the lower abundance of anamorsin detected by mass spectrometry in +4-fish ( $\log_2FC = -1.195$ ;  $q = 4.806 \times 10^{-7}$ ) was mirrored by immunoblot

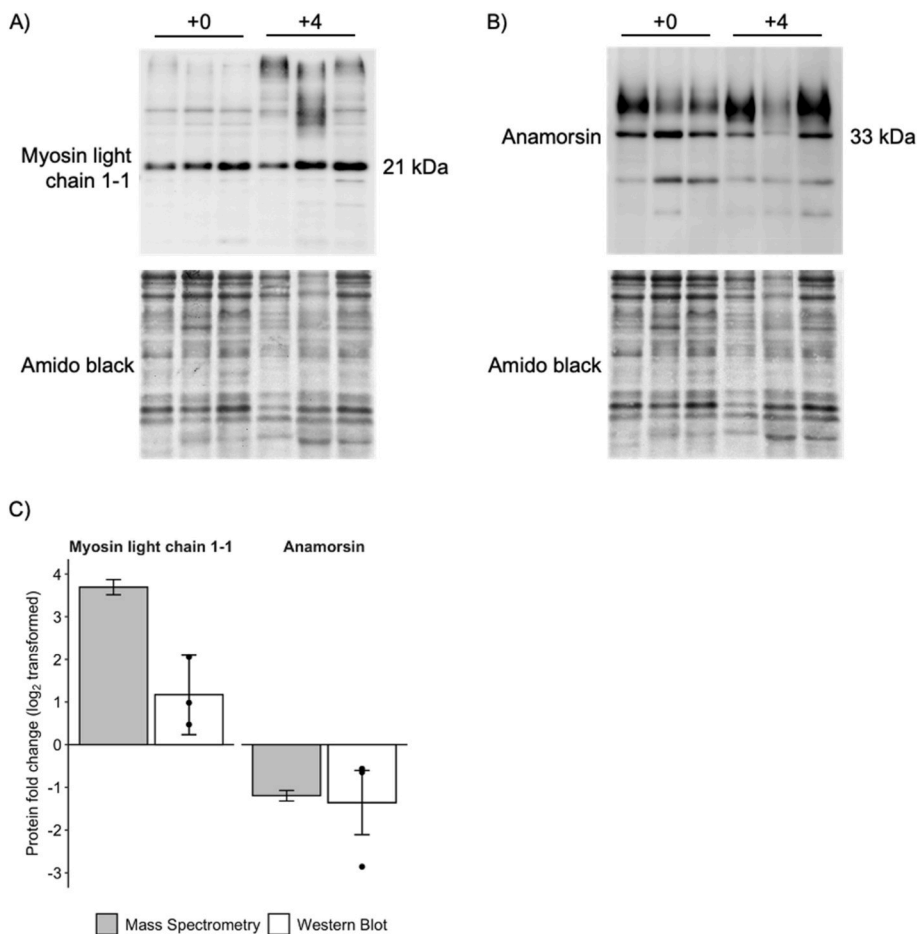


**Fig. 4.** Western blotting analysis of myosin light chain 1-1 and anamorsin abundance in the ventricles of juvenile Atlantic salmon (*Salmo salar*) raised in the two developmental treatments (+4 vs. +0). A) Western blot image showing single myosin light chain 1-1 band at 21 kDa for 3 biological replicates per developmental treatment, as well as the same blot stained for total protein using Amido black. B) Western blot image showing a band corresponding to anamorsin at 33 kDa for 3 biological replicates per developmental treatment, as well as the same blot stained for total protein using Amido black. C) Comparison of protein abundance as quantified by mass spectrometry (grey bars; N = 3) or Western blotting (white bars; N = 3). Data is mean fold change (log<sub>2</sub> transformed) ± SEM of protein abundance in the +4-group relative to the +0-control group. Additionally, individual data points for each biological replicate from Western blot analysis is shown.

analysis but did not reach statistical significance (log<sub>2</sub>FC = -1.355;  $p = 0.074$ ).

#### 4. Discussion

The heart is often considered the lynchpin of thermal performance in fishes, and is capable of remodelling to suit an organism's thermal environment. This temperature-dependent plasticity can involve changes in cardiac performance, heart morphology, and the cardiac proteome. We previously demonstrated that a 4°C increase in developmental temperature increased the cardiorespiratory thresholds for thermal performance in juvenile Atlantic salmon, as well as the proportion of compact myocardium within the heart. In the present study, we examined the ventricular proteomes of the same experimental fish. Selected differences in relative protein abundance are discussed below, with a particular focus on how they may contribute to the observed differences in thermal performance and myocardial morphology between developmental treatments.

##### 4.1. Protein homeostasis

Thermal stress is known to disrupt protein integrity, which can lead to an accumulation of misfolded and damaged proteins. Increased expression of molecular chaperones, particularly heat shock proteins, is a well documented response to thermal stress in fish (Anttila et al., 2014; Beemelmans et al., 2021a, 2021b; Jeffries et al., 2014; Jørgensen et al., 2014; Logan and Somero, 2011; Podrabsky and Somero, 2004). It is therefore not surprising that we observed higher protein abundance for two heat shock proteins (heat shock protein beta-2 and heat shock 70 kDa protein 9) in the +4-group. These differences may represent a rapid

heat shock response to the acute warming protocol. However, previous studies on the steady-state transcriptome of warm-acclimated salmonid hearts would suggest that this represents a sustained, long-term response to a warmer thermal environment, which can pre-condition fish to handle thermal stress events (Jørgensen et al., 2014; Vornanen et al., 2005).

When proteins cannot be repaired by molecular chaperones, they are selectively degraded via lysosomal autophagy or the ubiquitin-proteasome system (Wang and Robbins, 2014). Interestingly, we observed a downregulation of proteins associated with the ubiquitin-proteasome system in the +4-group relative to control fish. This finding is somewhat surprising given that protein turnover is critical to maintaining homeostasis under elevated temperature conditions, and protein degradation pathways are often upregulated in more thermally tolerant fish (O'Brien et al., 2018; Jayasundara et al., 2015; Logan and Somero, 2010). However, we did observe higher abundance of CREG1 in the +4-group, which is thought to play a cardioprotective role in the mammalian heart by activating lysosomal autophagy and antagonizing cardiac fibrosis (Song et al., 2017; Yan et al., 2015). Thus, it is likely that an increased abundance of heat shock proteins and lysosomal proteolysis of damaged proteins are sufficient to maintain protein homeostasis in the hearts of +4-fish.

##### 4.2. Metabolism

The vertebrate heart is a highly oxidative organ requiring high rates of aerobic ATP production to sustain its continuous contractile work (Driedzic & Gesser, 1994). Decreased expression of metabolic enzymes is sometimes observed with warm-acclimation in fish, which is thought to compensate for temperature-dependent increases in enzymatic rate



(Jayasundara et al., 2013). However, studies examining the hearts of warm-acclimated fish with higher acute thermal tolerances have also found an increase in the abundance of oxidative enzymes (Jayasundara et al., 2015; Jayasundara and Somero, 2013) and increased capacities for mitochondrial respiration, including in Atlantic salmon (Gerber et al., 2020). In the present study, the most strongly enriched subset of proteins showing higher abundance in +4-fish were those associated with the mitochondrial electron transport system (ETS). Increased abundance of ETS proteins per gram of tissue may indicate a higher mitochondrial density and increased oxidative capacity in the hearts of +4-fish. We also observed higher abundances of two TCA cycle proteins in the +4-group, while two proteins associated with anaerobic carbohydrate metabolism showed lower abundances.

Similar shifts in metabolic protein abundance were observed in the eurythermal goby *Gillichthys mirabilis* following acclimation from 13°C to 19°C, such that proteins involved in the TCA cycle and oxidative phosphorylation were more abundant in the hearts of warm-acclimated fish (Jayasundara et al., 2015). Similarly, a comparison of Antarctic fishes found that cardiac tissue from the more thermally tolerant *Notthenia coriiceps* species had a higher capacity for aerobic ATP-production compared to the less tolerant *Chaenocephalus aceratus* (O'Brien et al., 2018). This improved performance coincided with an increase in mitochondrial protein abundance. The increased abundance of proteins involved in oxidative metabolism may therefore indicate an improved capacity for aerobic ATP-production in the myocardium of +4-fish. Paired with an improved oxygen-delivery system to the myocardium, this may partly explain how +4-fish maintain cardiac function to higher temperatures than control fish.

#### 4.3. Vascularization

We previously reported that the hearts of +4-fish contained greater proportions of compact myocardium (Muir et al., 2021a), which receives an oxygen-rich coronary blood supply. Here, we identified angiogenesis-associated cell signaling proteins that were more abundant in the hearts of +4-fish. We additionally observed higher abundance of cell adhesion molecules associated with the vasculature in the +4-group. For example, collagen type-VIII is expressed in blood vessel endothelia and promotes vessel wall integrity (Robertson and Watton, 2013; Shuttleworth, 1997). The dystroglycan complex, which limits activity-induced myocardial damage, is also thought to promote angiogenesis (Hosokawa et al., 2002; Michele et al., 2009). Increased abundance of angiogenic proteins may simply reflect the higher proportion of vascularized compact myocardium in the ventricular tissue of +4-fish, or could reflect an induction of further capillarization within the compact myocardium in response to the higher oxygen demands of a warmer thermal environment. Warm-acclimation has been shown to induce capillarization in the hearts of juvenile Arctic charr (Anttila et al., 2015), and increase the expression of the angiogenic factor vascular endothelial growth factor (VEGF) in adult Atlantic salmon (Jørgensen et al., 2014). While we did not detect an increase in VEGF, we identified other candidate proteins which may support capillarization during environmental remodelling of the teleost heart (ribonuclease-like 3, S100-A16, and protein-glutamine gamma-glutamyltransferase 2). As recent studies have highlighted the importance of the coronary blood supply for maintaining cardiac function during heat exposure (Ekström et al., 2017, 2019; Morgenroth et al., 2021), improved vascularization of the myocardium may contribute to the improved thermal performance of +4-fish.

#### 4.4. Cardiac hypertrophy

In the present study, we provide molecular evidence that cardiomyocyte hypertrophy may contribute to our previously observed expansion of compact myocardium in the ventricles of +4-fish (Muir et al., 2021a). A hypertrophic model of cardiac growth is supported by

the increased abundance of some troponin-complex proteins in the +4-group, as this suggests that additional contractile machinery is being added to existing cardiomyocytes. Notably, we observed large increases in the abundance of tropomyosin alpha-1 and myosin light chain 1-1. Increased expression of  $\alpha$ -tropomyosin and the myosin light chains is regularly observed with cardiac hypertrophy in mammals (Lim et al., 2001; Swynghedauw, 1999). Meanwhile, the sarcomere organizing protein myozenin 2, which is a known repressor of cardiac hypertrophy in the mammalian heart (Osio et al., 2007), had lower abundance in our +4-fish compared to the controls.

A hypertrophic model of cardiac growth is further supported by the increased abundance of ribosomal proteins in the hearts of +4-fish. Increasing the capacity for protein synthesis is essential for compensatory hypertrophy (Hannan et al., 2003), and genes encoding ribosomal proteins were similarly upregulated during cold-induced hypertrophy of the trout heart (Vornanen et al., 2005). The increased abundance of proteins related to mitochondrial protein synthesis (28S ribosomal protein S14) and import (mitochondrial import inner membrane translocase subunit TIM13) further support the notion of increased mitochondrial capacity in the hearts of +4-fish. Indeed, TIM13 was similarly upregulated in the hearts of Antarctic icefish with higher thermal tolerance (O'Brien et al., 2018).

#### 4.5. Cardiac pathology

Cardiovascular disease is an increasing problem in salmonid aquaculture and poses a significant threat to animal health and welfare (Brijs et al., 2020; Frisk et al., 2020; Poppe et al., 2002, 2003). Recently, studies have linked rapid development under elevated temperatures to increased prevalence of cardiac deformities and upregulated markers of mammalian cardiac pathology (Brijs et al., 2020; Frisk et al., 2020). In Atlantic salmon, rapid smolt production under elevated rearing temperatures resulted in larger, more rounded ventricles that exhibited maladaptive thickening of the compact myocardium, as well as increased expression of signature markers of pathological cardiac hypertrophy (ANP and BNP; Frisk et al., 2020). While the changes in protein abundance observed here suggest a hypertrophic expansion of the compact myocardium in +4-fish, we did not detect differences in the typical markers of pathological hypertrophy (ANP, BNP, RCAN1, etc.). Further, +4-fish did not display larger or more rounded ventricles in our previous study, nor did they display impaired ventricular function when examined using Doppler echocardiography (Muir et al., 2021a). As noted by Frisk et al. (2020), the cardiac phenotype observed in 'fast smolts' reared at higher temperatures resembles the cortisol-mediated cardiac remodelling previously described in farmed salmonids (Johansen et al., 2011, 2017). Thus, it is likely that a range of stressors—such as overcrowding, handling and transportation, and poor water quality (Conte, 2004)—contribute to the development of pathological cardiac remodelling in intensive aquaculture, rather than temperature alone.

However, while the typical markers of cardiac pathology were not upregulated in our study, we did observe increased abundance of tetranectin in the hearts of +4-fish. Tetranectin promotes muscle cell differentiation during embryonic development, but re-expression in the adult heart has been associated with pathological cardiac fibrosis in mammals (McDonald et al., 2020; Wewer et al., 1998). To our knowledge, this is the first time that tetranectin has been implicated in remodelling of the teleost heart and further investigations into its role are therefore warranted.

#### 4.6. Study limitations

In the present study, cardiac tissue was collected from juvenile salmon following thermal performance trials, in order to confirm that developing in a warmer thermal environment had conferred an advantage in upper thermal tolerance. Given this study design, we cannot definitively distinguish between constitutive and acute effects of

temperature on differences in protein abundance between developmental groups. However, similar changes in the abundance of proteins involved in aerobic metabolism and protein homeostasis have previously been observed in steady-state examinations of warm-acclimated fish (Jayasundara et al., 2015). Given the short duration of the exposure to acute warming (60–90 min), it is unlikely that substantive changes in protein expression would occur during this timeframe. Even in the case of heat shock-inducible genes, changes at the protein level are not usually detected for at least 2 h (Mahat et al., 2016). While future studies will be valuable in teasing apart chronic versus acute responses to temperature in the cardiac proteome, this study holds significant value as the first description of the ventricular proteome in juvenile Atlantic salmon. Many studies have examined transcriptional responses to elevated temperature in the teleost heart (Anttila et al., 2014; Jayasundara et al., 2013; Jørgensen et al., 2014; Vornanen et al., 2005); however, few studies have examined changes to the cardiac proteome (Jayasundara et al., 2015; O'Brien et al., 2018).

## 5. Conclusions

In conclusion, this study provides the first proteomic analysis of the molecular mechanisms supporting temperature-induced cardiac phenotypes in juvenile Atlantic salmon. We previously demonstrated that fish exposed to a warmer thermal environment throughout development (+4°C) displayed increased proportions of compact myocardium within their hearts and maintained cardiac function to higher temperatures during acute warming (Muir et al., 2021a). Here, we observed changes in protein abundance that support a hypertrophic model of compact myocardium growth, as well as capillarization of the compact myocardium in +4-fish. We also report temperature-induced changes in proteins related to oxidative metabolism and protein homeostasis, suggesting a role for these processes in mediating thermal plasticity of cardiac function. Altogether, the increased abundance of proteins involved in oxidative metabolism, along with an expanded compact myocardium undergoing angiogenesis, suggest an enhanced energetic support system in the hearts of fish reared in a warmer thermal environment. We did not detect increases in the signature markers of cardiac pathology in the present study, nor do these fish display the functional and morphological indicators of cardiomyopathy reported in previous studies (Muir et al., 2021a; Frisk et al., 2020; Johansen et al., 2017). Thus, these temperature-dependent changes in the cardiac phenotype appear to represent adaptive plasticity and may contribute to the improved thermal performance of +4-fish. However, investigations into how this cardiac phenotype changes with age, particularly sexual maturation, would be fruitful.

## CRedit authorship contribution statement

**Carlisle A. Muir:** Conceptualization, Investigation, Formal analysis, Writing – original draft. **Bradley S. Bork:** Formal analysis, Validation, Visualization, Writing – review & editing. **Bryan D. Neff:** Conceptualization, Resources, Writing – review & editing, Supervision. **Sashko Damjanovski:** Conceptualization, Resources, Writing – review & editing, Supervision.

## Declaration of competing interest

The authors declare that they have no known competing financial interests or personal relationships that could have appeared to influence the work reported in this paper.

## Acknowledgements

This work was supported by Natural Sciences and Engineering Research Council (NSERC) Discovery Grants (RGPIN-2017-06045 to BDN and RGPIN-2018-06665 to SD) and a Strategic Project Grant

(494220-2016 STPGP to BDN). CAM and BSB were supported by NSERC Scholarships.

## Appendix A. Supplementary data

Supplementary data to this article can be found online at <https://doi.org/10.1016/j.crphys.2022.07.005>.

## References

- Anttila, K., Eliason, E.J., Kaukinen, K.H., Miller, K.M., Farrell, A.P., 2014. Facing warm temperatures during migration: cardiac mRNA responses of two adult *Oncorhynchus nerka* populations to warming and swimming challenges. *J. Fish. Biol.* 84, 1439–1456. <https://doi.org/10.1111/jfb.12367>.
- Anttila, K., Lewis, M., Prokkola, J.M., Kanerva, M., Seppanen, E., Kolari, I., Nikinmaa, M., 2015. Warm acclimation and oxygen depletion induce species-specific responses in salmonids. *J. Exp. Biol.* 218, 1471–1477. <https://doi.org/10.1242/jeb.119115>.
- Beemelmanns, A., Zanuzzo, F.S., Sandrelli, R.M., Rise, M.L., Gamperl, A.K., 2021a. The Atlantic Salmon's stress- and immune-related transcriptional responses to moderate hypoxia, an incremental temperature increase, and these challenges combined. *G3 Genes, Genomes, Genet.* 11 <https://doi.org/10.1093/g3journal/jkab102>.
- Beemelmanns, A., Zanuzzo, F.S., Xue, X., Sandrelli, R.M., Rise, M.L., Gamperl, A.K., 2021b. The transcriptomic responses of Atlantic salmon (*Salmo salar*) to high temperature stress alone, and in combination with moderate hypoxia. *BMC Genom.* <https://doi.org/10.1186/s12864-021-07464-x>.
- Bernardo, B.C., Weeks, K.L., Pretorius, L., McMullen, J.R., 2010. Molecular distinction between physiological and pathological cardiac hypertrophy: experimental findings and therapeutic strategies. *Pharmacol. Ther.* 128, 191–227. <https://doi.org/10.1016/j.pharmthera.2010.04.005>.
- Brijs, J., Hjelmstedt, P., Berg, C., Johansen, I.B., Sundh, H., Roques, J.A.C., Ekström, A., Sandblom, E., Sundell, K., Olsson, C., Axelsson, M., Gräns, A., 2020. Prevalence and severity of cardiac abnormalities and arteriosclerosis in farmed rainbow trout (*Oncorhynchus mykiss*). *Aquaculture* 526, 735417. <https://doi.org/10.1016/j.aquaculture.2020.735417>.
- Castro, V., Grisdale-Helland, B., Helland, S.J., Torgersen, J., Kristensen, T., Claireaux, G., Farrell, A.P., Takle, H., 2013. Cardiac molecular-acclimation mechanisms in response to swimming-induced exercise in Atlantic salmon. *PLoS One* 8, 1–10. <https://doi.org/10.1371/journal.pone.0055056>.
- Conte, F.S., 2004. Stress and the welfare of cultured fish. *Appl. Anim. Behav. Sci.* 86, 205–223. <https://doi.org/10.1016/J.APPLANIM.2004.02.003>.
- Davie, P.S., Farrell, A.P., 1991. The coronary and luminal circulations of the myocardium of fishes. *Can. J. Zool.* 69 <https://doi.org/10.1139/z91-278>, 1993–2001.
- Dindia, L.A., Alderman, S.L., Gillis, T.E., 2017. Novel insights into cardiac remodelling revealed by proteomic analysis of the trout heart during exercise training. *J. Proteomics* 161, 38–46. <https://doi.org/10.1016/j.jprot.2017.03.023>.
- Driedzic, W.R., Gesser, H., 1994. Energy metabolism and contractility in ectothermic vertebrate hearts: hypoxia, acidosis, and low temperature. *Physiol. Rev.* 74 (1), 221–258.
- Ekström, A., Axelsson, M., Gräns, A., Brijs, J., Sandblom, E., 2017. Influence of the coronary circulation on thermal tolerance and cardiac performance during warming in rainbow trout. *Am. J. Physiol. Regul. Integr. Comp. Physiol.* 312, 549–558. <https://doi.org/10.1152/ajpregu.00536.2016>.
- Ekström, A., Gräns, A., Sandblom, E., 2019. Can't beat the heat? Importance of cardiac control and coronary perfusion for heat tolerance in rainbow trout. *J. Comp. Physiol. B Biochem. Syst. Environ. Physiol.* 189, 757–769. <https://doi.org/10.1007/s00360-019-01243-7>.
- Eliason, E.J., Anttila, K., 2017. *Temperature and the Cardiovascular System. Fish Physiology, The Cardiovascular System: Development, Plasticity, and Physiological Responses*, 1st36B. Elsevier Inc, pp. 235–297.
- Farrell, A.P., Eliason, E.J., Sandblom, E., Clark, T.D., 2009. Fish cardiorespiratory physiology in an era of climate change. The present review is one of a series of occasional review articles that have been invited by the Editors and will feature the broad range of disciplines and expertise represented in our Editorial. *Can. J. Zool.* 87, 835–851. <https://doi.org/10.1139/Z09-092>.
- Farrell, A.P., Gamperl, A.K., Hicks, J.M.T., Shiels, H.A., Jain, K.E., 1996. Maximum cardiac performance of rainbow trout (*Oncorhynchus mykiss*) at temperatures approaching their upper lethal limit. *J. Exp. Biol.* 199, 663–672.
- Farrell, A.P., Hammons, A.M., Graham, M.S., Tibbitts, G.F., 1988. Cardiac growth in rainbow trout, *Salmo gairdneri*. *Can. J. Zool.* 66, 2368–2373. <https://doi.org/10.1139/z88-351>.
- Frisk, M., Høyland, M., Zhang, L., Vindas, M.A., Øverli, Ø., Johansen, I.B., 2020. Intensive smolt production is associated with deviating cardiac morphology in Atlantic salmon (*Salmo salar* L.). *Aquaculture* 529, 735615. <https://doi.org/10.1016/j.aquaculture.2020.735615>.
- Gallaugh, P.E., Thorarensen, H., Kiessling, A., Farrell, A.P., 2001. Effects of high intensity exercise training on cardiovascular function, oxygen uptake, internal oxygen transport and osmotic balance in chinook salmon (*Oncorhynchus tshawytscha*) during critical speed swimming. *J. Exp. Biol.* 204, 2861–2872. <https://doi.org/10.1242/jeb.204.16.2861>.
- Gamperl, A.K., Ajiboye, O.O., Zanuzzo, F.S., Sandrelli, R.M., Peroni, E. de F.C., Beemelmanns, A., 2020. The impacts of increasing temperature and moderate hypoxia on the production characteristics, cardiac morphology and haematology of

- Atlantic Salmon (*Salmo salar*). *Aquaculture* 519, 734874. <https://doi.org/10.1016/J.AQUACULTURE.2019.734874>.
- Gamperl, A.K., Farrell, A.P., 2004. Cardiac plasticity in fishes: environmental influences and intraspecific differences. *J. Exp. Biol.* 207, 2539–2550. <https://doi.org/10.1242/jeb.01057>.
- Gerber, L., Clow, K.A., Mark, F.C., Gamperl, A.K., 2020. Improved mitochondrial function in salmon (*Salmo salar*) following high temperature acclimation suggests that there are cracks in the proverbial 'ceiling'. *Sci. Rep.* 10, 1–12.
- Goeminne, L.J.E., Gevaert, K., Clement, L., 2018. Experimental design and data-analysis in label-free quantitative LC/MS proteomics: a tutorial with MSqRob. *J. Proteomics* 171, 23–36. <https://doi.org/10.1016/j.jprot.2017.04.004>.
- Götz, S., García-Gómez, J.M., Terol, J., Williams, T.D., Nagaraj, S.H., Nueda, M.J., Robles, M., Talón, M., Dopazo, J., Conesa, A., 2008. High-throughput functional annotation and data mining with the Blast2GO suite. *Nucleic Acids Res.* 36, 3420–3435. <https://doi.org/10.1093/NAR/GKN176>.
- Graham, M.S., Farrell, A.P., 1992. Environmental influences on cardiovascular variables in rainbow trout, *Oncorhynchus mykiss* (Walbaum). *J. Fish. Biol.* 41, 851–858. <https://doi.org/10.1111/j.1095-8649.1992.tb02713.x>.
- Hannan, R., Jenkins, A., Jenkins, A.K., Brandenburger, Y., 2003. Cardiac hypertrophy: a matter of translation. *Clin. Exp. Pharmacol. Physiol.* 30, 517–527. <https://doi.org/10.1046/J.1440-1681.2003.03873.X>.
- Hassinen, M., Haverinen, J., Vornanen, M., 2008. Electrophysiological properties and expression of the delayed rectifier potassium (ERG) channels in the heart of thermally acclimated rainbow trout. *Am. J. Physiol. Regul. Integr. Comp. Physiol.* 295, 297–308. <https://doi.org/10.1152/ajpregu.00612.2007>.
- Hosokawa, H., Ninomiya, H., Kitamura, Y., Fujiwara, K., Masaki, T., 2002. Vascular endothelial cells that express dystroglycan are involved in angiogenesis. *J. Cell Sci.* 115, 1487–1496. <https://doi.org/10.1242/JCS.115.7.1487>.
- Ifitkar, F.I., Hickey, A.J.R., 2013. Do mitochondria limit hot fish hearts? Understanding the role of mitochondrial function with heat stress in *Notolabrus celidotus*. *PLoS One* 8, E64120.
- Intergovernmental Panel on Climate Change (IPCC), 2021. Climate Change 2021: The Physical Science Basis. Contribution of Working Group I to the Sixth Assessment Report of the Intergovernmental Panel on Climate Change. <https://www.ipcc.ch/report/sixth-assessment-report-working-group-i/>.
- Jayasundara, N., Gardner, L.D., Block, B.A., 2013. Effects of temperature acclimation on Pacific bluefin tuna (*Thunnus orientalis*) cardiac transcriptome. *Am. J. Physiol. Regul. Integr. Comp. Physiol.* 305, 1010–1020. <https://doi.org/10.1152/ajpregu.00254.2013>.
- Jayasundara, N., Somero, G.N., 2013. Physiological plasticity of cardiorespiratory function in a eurythermal marine teleost, the longjaw mudsucker, *Gillichthys mirabilis*. *J. Exp. Biol.* 216, 2111–2121. <https://doi.org/10.1242/jeb.083873>.
- Jayasundara, N., Tomanek, L., Dowd, W.W., Somero, G.N., 2015. Proteomic analysis of cardiac response to thermal acclimation in the eurythermal goby fish *Gillichthys mirabilis*. *J. Exp. Biol.* 218, 1359–1372. <https://doi.org/10.1242/jeb.118760>.
- Jeffries, K.M., Hinch, S.G., Sierocinski, T., Pavlidis, P., Miller, K.M., 2014. Transcriptomic responses to high water temperature in two species of Pacific salmon. *Evol. Appl.* 7, 286–300. <https://doi.org/10.1111/evo.12119>.
- Johansen, I.B., Lunde, I.G., Røsjø, H., Christensen, G., Nilsson, G.E., Bakken, M., Øverli, Ø., 2011. Cortisol response to stress is associated with myocardial remodeling in salmonid fishes. *J. Exp. Biol.* 214, 1313–1321. <https://doi.org/10.1242/jeb.053058>.
- Johansen, I.B., Sandblom, E., Skov, P.V., Gräns, A., Ekström, A., Lunde, I.G., Vindas, M.A., Zhang, L., Höglund, E., Frisk, M., Sjaastad, I., Nilsson, G.E., Øverli, Ø., 2017. Bigger is not better: cortisol-induced cardiac growth and dysfunction in salmonids. *J. Exp. Biol.* 220, 2545–2553. <https://doi.org/10.1242/jeb.135046>.
- Jørgensen, S., Castro, V., Krasnov, A., Tørgersen, J., Timmerhaus, G., Hevrøy, E., Hansen, T., Susort, S., Breck, O., Takle, H., 2014. Cardiac responses to elevated seawater temperature in Atlantic salmon. *BMC Physiol.* 14, 2. <https://doi.org/10.1186/1472-6793-14-2>.
- Keen, A.N., Fenna, A.J., McConnell, J.C., Sherratt, M.J., Gardner, P., Shiels, H.A., 2016. The dynamic nature of hypertrophic and fibrotic remodeling of the fish ventricle. *Front. Physiol.* 427. <https://doi.org/10.3389/FPHYS.2015.00427>, 0.
- Keen, A.N., Klaiman, J.M., Shiels, H.A., Gillis, T.E., 2017. Temperature-induced cardiac remodeling in fish. *J. Exp. Biol.* <https://doi.org/10.1242/jeb.128496>.
- Klaiman, J.M., Fenna, A.J., Shiels, H.A., Macri, J., Gillis, T.E., 2011. Cardiac remodeling in fish: strategies to maintain heart function during temperature change. *PLoS One* 6, e24464. <https://doi.org/10.1371/journal.pone.0024464>.
- Lim, D.-S., Roberts, R., Marian, A.J., 2001. Expression profiling of cardiac genes in human hypertrophic cardiomyopathy: insight into the pathogenesis of phenotypes. *J. Am. Coll. Cardiol.* 38, 1175.
- Logan, C.A., Somero, G.N., 2011. Effects of thermal acclimation on transcriptional responses to acute heat stress in the eurythermal fish *Gillichthys mirabilis* (Cooper). *Am. J. Physiol. Regul. Integr. Comp. Physiol.* 300, 1373–1383. <https://doi.org/10.1152/ajpregu.00689.2010>.
- Logan, C.A., Somero, G.N., 2010. Transcriptional responses to thermal acclimation in the eurythermal fish *Gillichthys mirabilis* (Cooper 1864). *Am. J. Physiol. Regul. Integr. Comp. Physiol.* 299, 843–852. <https://doi.org/10.1152/ajpregu.00306.2010>.
- Mahat, D.B., Salamanca, H.H., Duarte, F.M., Danko, C.G., Lis, J.T., 2016. Mammalian heat shock response and mechanisms underlying its genome-wide transcriptional regulation. *Mol. Cell* 62, 63–78. <https://doi.org/10.1016/J.MOLCEL.2016.02.025/ATTACHMENT/A26EB1EE-03F5-423E-8282-5D6A5E331AC4/MMC1.PDF>.
- McDonald, K., Glezeva, N., Collier, P., O'Reilly, J., O'Connell, E., Tea, I., Russell-Hallinan, A., Tonry, C., Pennington, S., Gallagher, J., Ledwidge, M., Baugh, J., Watson, C.J., 2020. Tetranectin, a potential novel diagnostic biomarker of heart failure, is expressed within the myocardium and associates with cardiac fibrosis. *Sci. Rep.* 10, 1–12. <https://doi.org/10.1038/s41598-020-64558-4>.
- Michele, D.E., Kabaeva, Z., Davis, S.L., Weiss, R.M., Campbell, K.P., 2009. Dystroglycan matrix receptor function in cardiac myocytes is important for limiting activity-induced myocardial damage. *Circ. Res.* 105, 984. <https://doi.org/10.1161/CIRCRESAHA.109.199489>.
- Morgenroth, D., McArley, T., Gräns, A., Axelsson, M., Sandblom, E., Ekström, A., 2021. Coronary blood flow influences tolerance to environmental extremes in fish. *J. Exp. Biol.* 224. <https://doi.org/10.1242/jeb.239970>.
- Muir, C.A., Neff, B.D., Damjanovski, S., 2021a. Temperature-dependent plasticity mediates heart morphology and thermal performance of cardiac function in juvenile Atlantic salmon (*Salmo salar*). *J. Exp. Biol.* <https://doi.org/10.1242/jeb.244305>. Accepted: JEXBIO/2022/244305.
- Muir, C.A., Neff, B.D., Damjanovski, S., 2021b. Adaptation of a mouse Doppler echocardiograph system for assessing cardiac function and thermal performance in a juvenile salmonid. *Conserv. Physiol.* 9, 1–11. <https://doi.org/10.1093/conphys/coab070>.
- Muñoz, N.J., Farrell, A.P., Heath, J.W., Neff, B.D., 2015. Adaptive potential of a Pacific salmon challenged by climate change. *Nat. Clim. Change* 5, 163–166. <https://doi.org/10.1038/nclimate2473>.
- O'Brien, K.M., Rix, A.S., Egginton, S., Farrell, A.P., Crockett, E.L., Schlauch, K., Wooley, R., Hoffman, M., Merriman, S., 2018. Cardiac mitochondrial metabolism may contribute to differences in thermal tolerance of red-and white-blooded Antarctic notothenioid fishes. *J. Exp. Biol.* 221. <https://doi.org/10.1242/jeb.177816>.
- Osio, A., Tan, L., Chen, S.N., Lombardi, R., Nagueh, S.F., Shete, S., Roberts, R., Willerson, J.T., Marian, A.J., 2007. Myozenin 2 is a novel gene for human hypertrophic cardiomyopathy. *Circ. Res.* 100, 766. <https://doi.org/10.1161/01.RES.0000263008.66799.AA>.
- Podrabsky, J.E., Somero, G.N., 2004. Changes in gene expression associated with acclimation to constant temperatures and fluctuating daily temperatures in an annual killifish *Austrofundulus limnaeus*. *J. Exp. Biol.* 207, 2237–2254. <https://doi.org/10.1242/jeb.01016>.
- Poppe, T., Johansen, R., Gunnes, G., Tørud, B., 2003. Heart morphology in wild and farmed Atlantic salmon *Salmo salar* and rainbow trout *Oncorhynchus mykiss*. *Dis. Aquat. Org.* 57, 103–108. <https://doi.org/10.3354/dao057103>.
- Poppe, T.T., Johansen, R., Tørud, B., 2002. Cardiac abnormality with associated hernia in farmed rainbow trout *Oncorhynchus mykiss*. *Dis. Aquat. Org.* 50, 153–155. <https://doi.org/10.3354/DAO050153>.
- Pörtner, H.O., Knust, R., 2007. Climate change affects marine fishes through the oxygen limitation of thermal tolerance. *Science* (80) 315, 95–97. <https://doi.org/10.1126/science.1135471>.
- Robertson, A.M., Watton, P.N., 2013. Mechanobiology of the arterial wall. In: *Transport in Biological Media*. Elsevier, pp. 275–347. <https://doi.org/10.1016/B978-0-12-415824-5.00008-4>.
- Shiels, H.A., Di Maio, A., Thompson, S., Block, B.A., 2011. Warm fish with cold hearts: thermal plasticity of excitation–contraction coupling in bluefin tuna. *Proc. R. Soc. B Biol. Sci.* 278, 18–27. <https://doi.org/10.1098/RSPB.2010.1274>.
- Shuttleworth, C., 1997. Type VIII collagen. *Int. J. Biochem. Cell Biol.* 29, 75–81. [https://doi.org/10.1016/S1357-2725\(97\)00033-2](https://doi.org/10.1016/S1357-2725(97)00033-2).
- Simonot, D.L., Farrell, A.P., 2007. Cardiac remodeling in rainbow trout *Oncorhynchus mykiss* Walbaum in response to phenylhydrazine-induced anaemia. *J. Exp. Biol.* 210, 2574–2584. <https://doi.org/10.1242/JEB.004028>.
- Song, H., Yan, C., Tian, X., Zhu, N., Li, Y., Liu, D., Liu, Y., Liu, M., Peng, C., Zhang, H., Gao, E., Han, Y., 2017. CREG protects from myocardial ischemia/reperfusion injury by regulating myocardial autophagy and apoptosis. *Biochim. Biophys. Acta, Mol. Basis Dis.* 1863, 1893–1903. <https://doi.org/10.1016/J.BBADIS.2016.11.015>.
- Sticker, A., Goeminne, L., Martens, L., Clement, L., 2020. Robust summarization and inference in proteome-wide label-free quantification. *Mol. Cell. Proteomics* 19, 1209–1219. <https://doi.org/10.1074/mcp.RA119.001624>.
- Swynghedauw, B., 1999. Molecular mechanisms of myocardial remodeling. *Physiol. Rev.* 215–262. <https://doi.org/10.1152/PHYSREV.1999.79.1.215>.
- Tota, B., 1983. Vascular and metabolic zonation in the ventricular myocardium of mammals and fishes. *Comp. Biochem. Physiol., A Part A Physiol.* 76, 423–437. [https://doi.org/10.1016/0300-9629\(83\)90442-5](https://doi.org/10.1016/0300-9629(83)90442-5).
- Vornanen, M., Hassinen, M., Koskinen, H., Krasnov, A., 2005. Steady-state effects of temperature acclimation on the transcriptome of the rainbow trout heart. *Am. J. Physiol. Regul. Integr. Comp. Physiol.* 289, 1177–1184. <https://doi.org/10.1152/ajpregu.00157.2005>.
- Vornanen, M., Shiels, H.A., Farrell, A.P., 2002. Plasticity of excitation–contraction coupling in fish cardiac myocytes. *Comp. Biochem. Physiol. Part A Mol. Integr. Physiol.* 132, 827–846. [https://doi.org/10.1016/S1095-6433\(02\)00051-X](https://doi.org/10.1016/S1095-6433(02)00051-X).
- Wang, X., Robbins, J., 2014. Proteasomal and lysosomal protein degradation and heart disease. *J. Mol. Cell. Cardiol.* 16. <https://doi.org/10.1016/J.YJMCC.2013.11.006>, 0.
- Wewer, U., Iba, K., Durkin, M., Nielsen, F., Loechel, F., Gilpin, B., Kuang, W., Engvall, E., Albrechtsen, R., 1998. Tetranectin is a novel marker for myogenesis during embryonic development, muscle regeneration, and muscle cell differentiation in vitro. *Dev. Biol.* 200, 247–259. <https://doi.org/10.1006/DBIO.1998.8962>.
- Yan, C., Li, Y., Tian, X., Zhu, N., Song, H., Zhang, J., Sun, M., Han, Y., 2015. CREG1 ameliorates myocardial fibrosis associated with autophagy activation and Rab7 expression. *Biochim. Biophys. Acta* 353–364. <https://doi.org/10.1016/J.BBADIS.2014.05.027>, 1852.